

## B3LYP/6-311++G\*\* geometry-optimization study of pentahydrates of $\alpha$ - and $\beta$ -D-glucopyranose<sup>☆</sup>

Frank A. Momany,<sup>a,\*</sup> Michael Appell,<sup>b</sup> J. L. Willett<sup>a</sup> and Wayne B. Bosma<sup>c</sup>

<sup>a</sup>Plant Polymer Research, USDA, ARS, National Center for Agricultural Utilization Research, 1815 N. University St., Peoria, IL 61604, USA

<sup>b</sup>Mycotoxin Research, USDA, ARS, National Center for Agricultural Utilization Research, 1815 N. University St., Peoria, IL 61604, USA

<sup>c</sup>Department of Chemistry and Biochemistry, Bradley University, Peoria, IL 61625, USA

Received 23 November 2004; accepted 20 April 2005

**Abstract**—Five water molecules were placed in 37 different configurations around  $\alpha$ - and  $\beta$ -D-glucopyranose in the *gt*, *gg*, and *tg* conformational states, and the glucose–water complexes were geometry optimized using density functionals at the B3LYP/6-311++G\*\* level of theory. The five water molecules were organized in space and energy minimized using an empirical potential, AMB02C, and then further geometry optimized using DFT algorithms to minimum energy positions. Electronic energy, zero point vibrational energy, enthalpy, entropy, stress energy on glucose and the water cluster, hydrogen-bond energy, and relative free energy were obtained for each configuration using thermodynamic procedures and an analytical Hessian program. The lowest energy complex was that of a clustering of water molecules around the 1- and 6-hydroxyl positions of the  $\beta$ -*gt* anomer. Configurations in which the water molecules created a favorable network completely around and under glucose were found to have low energy for both  $\alpha$  and  $\beta$  anomers. Calculation of the  $\alpha/\beta$  anomeric ratio using the zero point corrected energy gave,  $\sim 32/68\%$ , highly favoring the  $\beta$  anomer in agreement with the experimental  $\sim 36/64\%$  value. This ratio is better than the  $\sim 50/50\%$  ratio found in our previous monohydrate study. An approximate hydroxymethyl population was obtained by noting average relative energies among the three conformational states, *gt*, *gg*, and *tg*. In the  $\beta$  anomer complexes the *gt* conformation was favored over the *gg* state, while in the  $\alpha$  anomer complexes the *gg* state was favored over the *gt* conformation, with the *tg* conformations all being of higher energy making little or no contribution to the rotamer population. Some geometry variances, found between glucose in vacuo and glucose after interaction with water molecules, are described and account for some observed C-5–C-6 bond length anomalies reported by us previously for the vacuum glucose structures.

Published by Elsevier Ltd.

**Keywords:** B3LYP/6-311++G\*\*; Glucose; Pentahydrates; Relative free energy; Entropy; Hydrogen bonds

### 1. Introduction

All natural carbohydrate chemistry takes place in water; that makes it imperative to understand how water molecules interact with the many hydroxyl groups available

in sugars, and to further understand how specific interactions modify the conformational and configurational characteristics of these important natural products. Clearly, the interactions between water and carbohydrate molecules are directly related to their antifreezing and plasticizing properties, which are important in order to understand, for example, their utility in food applications, their protective effect for cryobiological applications, and their ability to produce useful protective films.

Little high-level computational work on hydrated carbohydrates has been published in which site-specific hydroxyl–water interactions are considered in detail.

<sup>☆</sup>Names are necessary to report factually on available data; however, the USDA neither guarantees nor warrants the standard of the product, and the use of a name by USDA implies no approval of the product to the exclusion of others than may also be suitable.

\*Corresponding author. Tel./fax: +1 309 681 6362; e-mail: [momanyfa@ncaur.usda.gov](mailto:momanyfa@ncaur.usda.gov)

This work is a continuation of work presented in a previous paper<sup>1</sup> in which we described calculations carried out on monohydrate complexes of  $\alpha$ - and  $\beta$ -D-glucopyranose using the B3LYP density functionals and the 6-311++G\*\* basis set. In Ref. 1, we presented data for one water molecule located at various energy-optimized positions around glucose. The region around the 1-position was of particular interest because these complexes were found to be of lowest relative energy, particularly when the water interacted with the 1-hydroxyl and 5-ether oxygen. The complexes with the water molecules near the 2-, 3-, 4-, and 6-hydroxyl positions were generally less energetically favorable than those near the 1-position.<sup>1</sup> Of further interest was the effect of water on the anomeric ratio. Analysis of the calculated  $\alpha/\beta$  anomeric ratio for the monohydrates<sup>1</sup> and glucose in vacuo<sup>2</sup> showed that the addition of a water molecule decreased the  $\alpha/\beta$  anomeric ratio from  $\sim 60/40\%$  to  $50/50\%$ , making a significant step toward the experimental (solution phase) ratio of  $36/64\%$ . In this study we calculate the anomeric population with five water molecules around the glucose molecule, again paying particular attention to the 1- and 6-positions as well as water distributed in other local minima around the molecule. Further, we are now able to examine, in an approximate manner, the distribution of hydroxymethyl orientations as the O-6–H-6 hydroxyl group now interacts with water molecules for a number of configurations and with different conformations of the hydroxymethyl group.

Even though considerable literature exists that describes semiempirical molecular orbital, density functional (DFT), and HF ab initio calculations on the glucose molecule in vacuo,<sup>3–19</sup> there have been relatively few treatments where explicit water molecules were included, our previous glucose monohydrate DFT study<sup>1</sup> of 26 complexes being the most complete monohydrate study to date. Some glucose–water heterodimer single state configuration calculations<sup>20,21</sup> have also taken water explicitly into account during geometry optimization. The semiempirical inclusion of solvent by use of solvent free-energy methods<sup>5–7</sup> is clearly not the same as the explicit inclusion of water molecules in the DFT calculations, where we obtain detailed structural and energetic information. It is not claimed here that five water molecules are sufficient to mimic bulk solvent. However, our goal is to examine how adding more than one water molecule influences the internal energy and geometry of the carbohydrate, for example, by changing the hydroxyl rotamer positions and how these geometry changes affect the energetics of the hydrated complex.

Although the monohydrate study suggested that entropy plays a significant role in anomeric preference, it was also found that when the ring of exocyclic intramolecular hydrogen bonds around glucose were broken, the total energy of the complex increased. This is particularly true when the 2-hydroxyl group is rotated away

from the direction of the 1-hydroxyl toward a water molecule in the  $\alpha$  anomer. From this result we speculated that the  $\beta$  anomer could become energetically favored if water approached the 2-position and caused significant conformational distortion at this position. This observation was significant because it led to this work, where more water molecules are included. A possible explanation of the C-5–C-6 bond shortening observed in experimental carbohydrate structures but not found previously in our in vacuo glucose computational studies is presented.

It may not be possible to explain all of the glucose anomalies with so few water molecules since it is thought<sup>22</sup> that the number of water molecules forming the first solvation shell around glucose is  $\sim 8$ – $10$ . However, by the study of different positions of the five water molecules around glucose, different regions of the molecular surface are probed, and this allows some interpretation of the effect of the hydration layer at specific sites.

## 2. Experimental

### 2.1. Computational methods

In this work DFT methods (B3LYP/6-31+G\* followed by B3LYP/6-311++G\*\*) were used to geometry optimize selected pentahydrates of the  $\alpha$  and  $\beta$  anomers of the *gg*, *gt*, and *tg* conformers of glucose starting from configurations obtained by energy minimization using a revised version (AMB02C) of the published (AMB99C) force field.<sup>23,24</sup> Several cycles of empirical energy minimization and molecular dynamics were carried out on the pentahydrates to find low-energy complex structures. Selected glucose configurations were carried through molecular dynamics simulations of periodic cells filled with TIP3P water molecules, and the hydration shell around the glucose molecule was studied for possible preferred sites for five water molecules. The DFT calculations were intensive and required additional geometry-optimization cycles at the higher basis set even after optimization at the smaller basis sets. Although the water molecules did not move significantly from the positions found using the empirical potentials, it was clear that some small readjustments in orientation and position occurred upon optimization. This is to be expected, as many water–water interactions are removed when the pentahydrate is selected from a box of water molecules. In several cases the reorientation resulted in a configuration similar to one found previously, suggesting a common structural motif at different sites around the glucose molecule.

The B3LYP nonlocal exchange correlation functionals<sup>25,26</sup> and two basis sets, denoted 6-31+G\* and 6-311++G\*\* were used as described previously for glucose,<sup>1,2</sup> maltose,<sup>27</sup> and cellobiose.<sup>28,29</sup> In this work,

the NUMHES program was used to obtain a preliminary Hessian from semiempirical software, followed by preliminary geometry optimization of from 50 to 100 cycles of energy minimization carried out at the B3LYP/6-31+G\* level. Geometry optimization was then continued with the larger triple valence basis set. The use of 6-31+G\* as a starting basis set has been found to be more efficient and results in better carbohydrate geometry than the 6-31G\* basis set used previously.<sup>27</sup> In particular, the C–O–H angle, hydrogen-bond distances, and energies are better described by the 6-31+G\* basis set than the 6-31G\* basis set<sup>27</sup> when used with the B3LYP density functional. Geometry optimization was considered satisfactory if energy differences between cycles of optimization were less than  $1 \times 10^{-6}$  Hartree and a gradient of less than  $1 \times 10^{-4}$  au was achieved. In order to get useful thermodynamic properties for these very complex structures, a full analytical Hessian calculation (HESS) was carried out on each geometry-optimized structure, both Hessian and optimization being at the B3LYP/6-311++G\*\* level of theory. The Hessian matrix built up only from geometry-optimization cycles results in large variances in thermodynamic values and was therefore not used to determine the vibrational frequencies and thermodynamic data.

The density functional, basis set, and analytical Hessian were programs included in the Parallel Quantum Solutions (PQS version 3.1) software.<sup>30</sup> Parallel Quantum Solutions QS4-2000S, and QS4-2400S hardware was used for all DFT calculations. Vibrational frequencies were calculated after geometry optimization and after the analytical Hessian calculation at the larger basis set, as was the zero point energy, stress energy,

enthalpy, entropy, and relative or Gibbs free energy for each complex. The thermodynamic parameters listed in the tables are those obtained after calculation of the analytical Hessian at the B3LYP/6-311++G\*\* level of theory. Cartesian coordinates of the complexes are available from the authors.

### 3. Results

The description of the glucopyranose pentahydrate energetics and energy related to number of hydrogen bonds is presented in Tables 1, 3, 5, 7 and 9, while Tables 2, 4, 6, 8 and 10 give selected bond lengths and angles for the  $\alpha$  and  $\beta$  anomers. The higher energy *tg* conformations are generally not populated in solution; accordingly, fewer *tg* hydrates were calculated than for the *gt* and *gg* rotamers.

#### 3.1. $\alpha$ -*gt* Conformations

In configuration  $\alpha$ -*gt*-I, the positions of water molecules after optimization are as shown in Figure 1. The OH-1 proton donor interaction to a water oxygen atom is complicated by the interaction of that water's hydrogen atom acting as a donor to a second water's oxygen atom, and its subsequent donor interaction with the hydroxymethyl group's O-6 oxygen. The two short hydrogen-bond distances (see Fig. 1) of  $\sim 1.74$  Å suggest strong interactions around the OH-1 position. However, the other water molecules' hydrogen bonds ( $\sim 1.80$ – $1.97$  Å) are longer, the net effect being that the average hydrogen-bond energy is quite strong ( $\sim -8.5$  kcal/mol) (see

**Table 1.** B3LYP/6-311++G\*\* geometry-optimized energies (kcal/mol) and analytical Hessian-derived thermodynamic parameters for the *gt* form of  $\alpha$ -D-glucopyranose pentahydrate

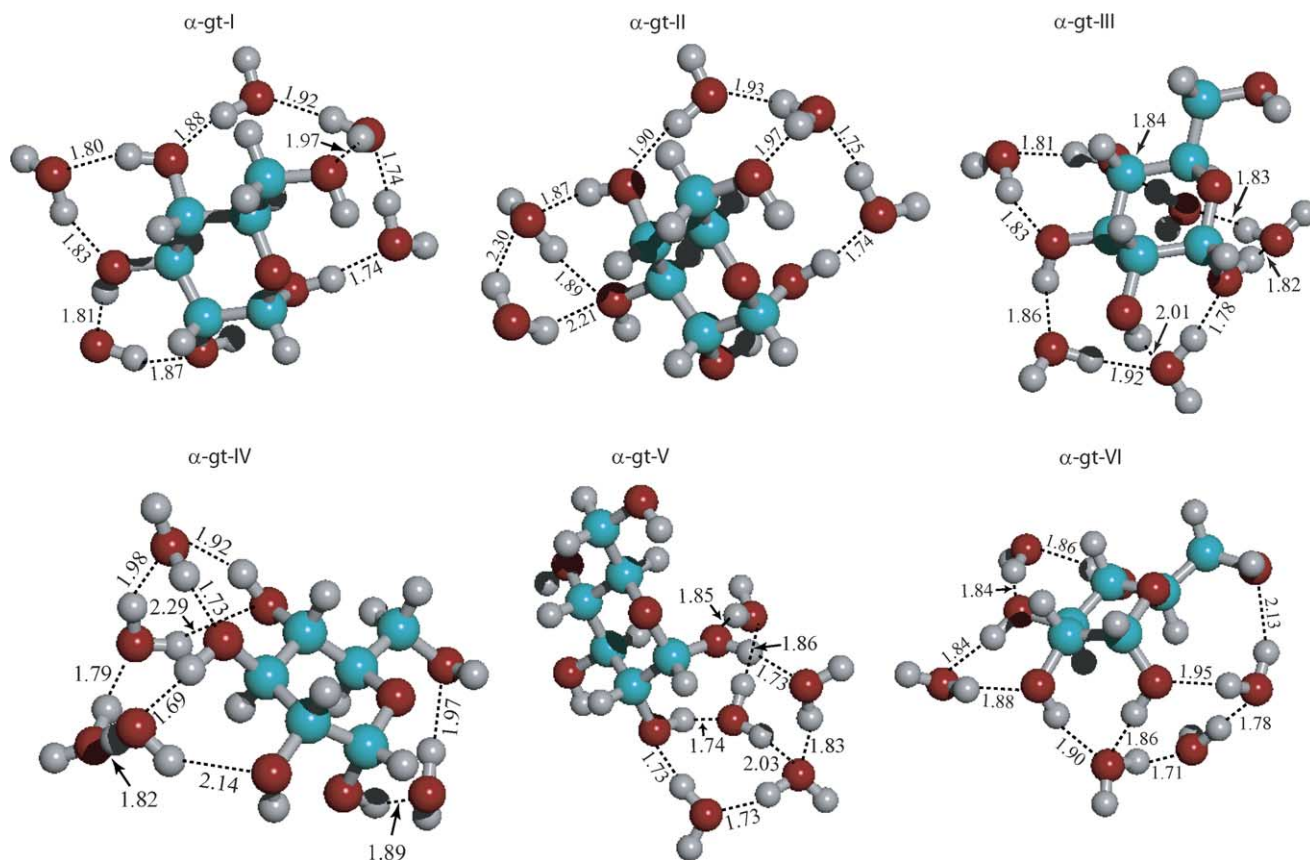
	$\alpha$ - <i>gt</i> Conformations					
	$\alpha$ - <i>gt</i> -I	$\alpha$ - <i>gt</i> -II	$\alpha$ - <i>gt</i> -III	$\alpha$ - <i>gt</i> -IV	$\alpha$ - <i>gt</i> -V	$\alpha$ - <i>gt</i> -VI
<i>E</i>	−671,298.222	−671,293.181	−671,291.522	−671,296.335	−671,296.339	−671,293.097
$\Delta E$	1.380	6.420	8.079	3.266	3.262	6.505
ZPVE	203.623	203.253	203.047	203.782	203.094	203.807
$\Delta E$ ( <i>E</i> + ZPVE)	1.320	5.991	7.444	3.366	2.674	6.629
<i>E</i> glucose(st) <sup>a</sup>	−431,349.765	−431,350.350	−431,344.770	−431,348.956	−431,349.577	−431,341.364
$\Delta E$ (st − vac)glucose	3.661	3.076	8.656	4.470	3.849	12.062
<i>E</i> 5-waters(st)	−239,905.712	−239,906.194	−239,907.602	−239,912.876	−239,914.585	−239,905.604
$\Delta E$ (st − vac)water	−13.417	−13.899	−15.307	−20.581	−22.290	−13.309
$\Delta E$ (total <i>E</i> − st mols)	−42.744	−36.637	−39.150	−34.503	−32.177	−46.129
Enthalpy ( <i>H</i> )	220.175	220.214	219.950	220.269	219.840	220.314
<i>S</i> (cal/mol K)	170.124	174.380	172.203	170.008	172.225	170.374
<i>E</i> (Hyd. bond Ave.) <sup>b</sup>	−8.548	−7.328	−7.830	−6.901	−6.435	−9.226
<i>E</i> ( $\Delta E$ /# Hyd. bonds)	−6.106	−6.106	−5.593	−3.834	−8.044	−5.766
$\Delta G_{298}^{\circ}$	1.376	5.188	7.232	3.492	2.498	6.566

<sup>a</sup> The stressed (st) energy refers to the energy of the isolated molecule in the same geometry as it has in the complex. The vacuum (vac) energy of the molecule refers to the energy of the molecule in its energy minimized vacuum geometry. *E* (vac)  $\alpha$ -*gt* glucose = −431,353.426 kcal/mol, *E* (vac)-water = −47,978.459 kcal/mol  $\times$  5-waters = −239,892.295 kcal/mol, st mols = st glucose + st water.

<sup>b</sup> Hydrogen (Hyd.) bond average is the  $\Delta E$  value divided by 5. This value includes only glucose–water interaction energies, the water–water interactions are included in the water-stressed value. Hydrogen bond energy is the stressed glucose plus stressed water subtracted from the total energy divided by the number of hydrogen bonds between waters and glucose.

**Table 2.** Selected B3LYP/6-311++G\*\* optimized internal coordinates for the *gt* form of  $\alpha$ -D-glucopyranose pentahydrates

	$\alpha$ - <i>gt</i> Conformations					
	$\alpha$ - <i>gt</i> -I	$\alpha$ - <i>gt</i> -II	$\alpha$ - <i>gt</i> -III	$\alpha$ - <i>gt</i> -IV	$\alpha$ - <i>gt</i> -V	$\alpha$ - <i>gt</i> -VI
<i>Bond lengths</i> ( $\text{\AA}$ )						
O-5-C-5	1.434	1.434	1.441	1.435	1.441	1.441
C-1-O-5	1.415	1.422	1.406	1.415	1.416	1.407
O-1-C-1	1.400	1.395	1.429	1.406	1.408	1.416
C-6-C-5	1.522	1.522	1.523	1.522	1.521	1.518
C-3-C-4	1.538	1.530	1.535	1.537	1.526	1.538
HO-1-O-1	0.987	0.987	0.982	0.978	0.983	0.974
<i>Bond angle</i> (deg)						
C-1-O-5-C-5	114.5	115.1	116.8	113.8	115.1	113.8
O-1-C-1-O-5	114.0	114.3	113.1	112.6	112.0	108.8
HO-1-O-1-C-1	112.6	112.4	113.5	109.7	109.9	113.5
O-5-C-5-C-4	111.0	111.7	113.4	109.1	109.7	109.3
O-5-C-5-C-6	105.7	105.6	105.4	105.8	105.9	106.6
HO-6-O-6-C-6	107.2	107.2	107.1	106.6	107.0	107.0
C-1-C-2-C-3	111.4	110.0	108.6	112.5	110.7	115.1
<i>Dihedral angle</i> (deg)						
HO-1-O-1-C-1-O-5	52.7	54.3	13.1	45.9	109.2	-140.3
HO-2-O-2-C-2-C-1	-37.3	-39.8	-63.2	-36.8	-63.9	-72.1
C-1-O-5-C-5-C-4	61.1	60.0	49.4	66.9	61.0	69.8
O-5-C-5-C-4-C-3	-51.7	-51.4	-43.6	-57.6	-55.2	-60.9
C-5-C-4-C-3-C-2	46.6	50.1	49.1	47.7	53.5	47.4
O-5-C-5-C-6-O-6	63.5	63.1	60.7	54.5	61.3	63.4
HO-6-O-6-C-6-C-5	-56.6	-57.7	-57.3	-71.9	-53.3	-66.8

**Figure 1.** Hydrogen-bonding configurations of water molecules about  $\alpha$ -*gt*.



**Table 3.** B3LYP/6-311++G\*\* geometry-optimized energies (kcal/mol) and analytical Hessian-derived thermodynamic parameters for the *gt* form of  $\beta$ -D-glucopyranose pentahydrate

	$\beta$ - <i>gt</i> Conformations								
	$\beta$ - <i>gt</i> -I	$\beta$ - <i>gt</i> -II	$\beta$ - <i>gt</i> -III	$\beta$ - <i>gt</i> -IV	$\beta$ - <i>gt</i> -V	$\beta$ - <i>gt</i> -VI	$\beta$ - <i>gt</i> -VII	$\beta$ - <i>gt</i> -VIII	$\beta$ - <i>gt</i> -IX
<i>E</i>	-671,294.230	-671,285.463	-671,294.150	-671,288.725	-671,289.418	-671,294.595	-671,299.601	-671,286.243	-671,294.457
$\Delta E$	5.371	14.138	5.451	10.876	10.183	5.006	0.000	13.358	5.144
ZPVE	203.315	201.317	203.310	202.322	202.210	203.192	203.682	202.004	202.607
$\Delta E$ ( <i>E</i> + ZPVE)	5.004	11.773	5.079	9.516	8.711	4.516	0.000	11.680	4.069
<i>E</i> glucose(st) <sup>a</sup>	-431,348.085	-431,349.447	-431,348.255	-41,349.327	-431,346.990	-431,349.053	-431,350.308	-431,343.311	-431,343.767
$\Delta E$ (st – vac)glucose	4.456	3.094	4.286	3.214	5.551	3.488	2.233	9.230	8.774
<i>E</i> 5-waters(st)	-239,905.949	-239,898.586	-239,905.891	-239,903.689	-239,906.320	-239,899.991	-239,918.003	-239,898.351	-239,914.422
$\Delta E$ (st – vac)water	-13.650	-6.291	-13.596	-11.394	-14.025	-7.696	-25.708	-6.056	-22.127
$\Delta E$ (total <i>E</i> – st mols)	-40.196	-37.430	-40.004	-35.709	-36.108	-45.551	-31.290	-44.581	-36.268
Enthalpy ( <i>H</i> )	220.258	218.846	220.271	219.758	219.669	219.927	220.112	219.463	218.998
<i>S</i> (cal/mol K)	173.306	182.638	173.207	180.437	180.136	171.879	168.185	179.152	170.196
<i>E</i> (Hyd. bond Ave.)	-8.039	-7.486	-8.001	-7.142	-7.222	-9.110	-6.258	-8.916	-7.254
<i>E</i> ( $\Delta E$ /# Hyd. bonds)	-5.742	-6.238	-5.715	-5.952	-4.514	-5.061	-7.823	-4.953	-7.254
$\Delta G_{298}^{\circ}$	4.503	9.077	4.625	7.383	6.690	4.232	0.512	9.953	3.943

See legends in Table 1.

<sup>a</sup> *E* (vac) $\beta$ -*gt* glucose = -431,352.541 kcal/mol, *E* (vac)water = -47,978.459 kcal/mol  $\times$  5-waters = -239,892.295 kcal/mol.

Table 1). A comparison of the  $\alpha$ -*gt*-I water configuration to that of conformers  $\beta$ -*gt*-I and  $\beta$ -*gt*-III is of interest as the water positions are similar in all three. In this case the  $\beta$  anomers are  $\sim 4$  kcal/mol higher in electronic energy than  $\alpha$ -*gt*-I. The reason for this may be found by examination of the HO-2–O-1 interaction in the  $\alpha$ -*gt*-I form. We find that the dihedral angle defined by HO-2–O-2–C-2–C-1 (see Table 2) is  $\sim -37^\circ$  as compared to that of the vacuum glucose value of  $\sim -44^\circ$ .<sup>2</sup> From this it appears that the particular configuration of water molecules is not putting stress on the HO-2–O-2–C-2–C-1 dihedral angle to change it significantly; because of this, the HO-2–O-1 hydrogen-bond distance of 2.087 Å remains short and allows the  $\alpha$ -*gt*-I configuration to retain a lower glucose molecular energy than the equivalent  $\beta$ -*gt* configurations, where this particular intramolecular interaction is much longer. This result is confirmed by examination of the glucose stress energies ( $\Delta E$  (st – vac)glucose) in Tables 1 and 3. The stress energy is the difference between the energy of the conformation after being perturbed by interaction with water molecules (st) and the vacuum (vac) optimized energy of the particular conformation.

The configuration,  $\alpha$ -*gt*-II, shown in Figure 1, also has a short hydrogen bond (1.74 Å) from the water oxygen to the 1-hydroxyl hydrogen. The difference of this configuration from  $\alpha$ -*gt*-I occurs at the 3- and 4-positions where the water molecules take up positions above and below the 3- and 4-hydroxyl groups. Since there is no water molecule interacting with the 2-hydroxyl group, the usually short HO-2...OH-1 hydrogen bond is near that length found in the vacuum study of glucose.<sup>2</sup> The loss of stability ( $\sim 5$  kcal/mol) of this configuration relative to  $\alpha$ -*gt*-I is a result of breaking the network of intramolecular interactions around the glucose ring, as shown also by the lower water–water energy in  $\alpha$ -*gt*-II relative to  $\alpha$ -*gt*-I. That is, the water bridge between the 2- and 3-hydroxyl groups in  $\alpha$ -*gt*-I is missing in  $\alpha$ -*gt*-II, although the three water molecules located under the 6-hydroxyl group connecting the 1-hydroxyl with a bridge to the 4-hydroxyl is retained in both configurations. The loss of the water bridge between 2- and 3-hydroxyl groups means that the 2-hydroxyl group is pulled back in  $\alpha$ -*gt*-II relative to  $\alpha$ -*gt*-I. This, in turn, results in a lengthening of the HO-2...O-1 hydrogen bond from 2.09 Å in  $\alpha$ -*gt*-I to 2.25 Å in  $\alpha$ -*gt*-II. The largest variance in hydroxyl dihedral angle occurs at the 3-hydroxyl position where the HO-3–O-3–C-3–C-2 dihedral angle is  $-45.9^\circ$  in  $\alpha$ -*gt*-II and  $-61.2^\circ$  in  $\alpha$ -*gt*-I. This is a result of the different water positions around the 3- and 4-hydroxyl groups. A large increase ( $\sim 0.016$  Å) in the C-3–O-3 bond length relative to that found in  $\alpha$ -*gt*-I, is found in this configuration, a result of having three hydrogen atoms (two from water molecules at 1.89 and 2.21 Å) interacting through hydrogen-bonding directed at the O-3 atom. Some shortening ( $\sim 0.012$  Å) of the  $\alpha$ -*gt*-II

**Table 4.** Selected B3LYP/6-311++G\*\* optimized internal coordinates for the *gt* form of  $\beta$ -D-glucopyranose pentahydrates

	$\beta$ - <i>gt</i> Conformations								
	$\beta$ - <i>gt</i> -I	$\beta$ - <i>gt</i> -II	$\beta$ - <i>gt</i> -III	$\beta$ - <i>gt</i> -IV	$\beta$ - <i>gt</i> -V	$\beta$ - <i>gt</i> -VI	$\beta$ - <i>gt</i> -VII	$\beta$ - <i>gt</i> -VIII	$\beta$ - <i>gt</i> -IX
<i>Bond lengths</i> (Å)									
O-5-C-5	1.425	1.439	1.425	1.439	1.429	1.444	1.429	1.437	1.438
C-1-O-5	1.425	1.422	1.425	1.420	1.417	1.433	1.422	1.408	1.416
O-1-C-1	1.383	1.405	1.383	1.405	1.403	1.393	1.395	1.394	1.396
C-6-C-5	1.521	1.520	1.521	1.522	1.525	1.524	1.523	1.527	1.522
C-3-C-4	1.546	1.530	1.546	1.529	1.545	1.540	1.530	1.538	1.538
HO-1-O-1	0.976	0.963	0.976	0.964	0.977	0.983	0.998	0.975	0.966
<i>Bond angle</i> (deg)									
C-1-O-5-C-5	110.0	113.7	110.0	113.3	111.8	113.1	112.5	114.7	113.5
O-1-C-1-O-5	110.5	107.5	110.4	107.6	107.4	107.9	108.4	104.6	108.8
HO-1-O-1-C-1	105.6	109.2	105.6	109.1	106.7	109.9	106.5	109.5	108.6
O-5-C-5-C-4	111.5	110.4	111.4	110.1	109.4	108.9	108.3	109.2	110.6
O-5-C-5-C-6	106.6	105.9	106.6	106.2	106.7	108.4	106.9	107.7	106.1
HO-6-O-6-C-6	106.7	107.2	106.7	107.4	107.6	109.1	109.0	108.6	107.2
C-1-C-2-C-3	108.7	108.9	108.8	108.8	111.1	110.4	109.1	111.4	109.7
<i>Dihedral angle</i> (deg)									
HO-1-O-1-C-1-O-5	-80.7	-75.5	-80.9	-75.0	-59.7	-72.4	-64.7	-161.2	60.4
HO-2-O-2-C-2-C-1	43.1	94.6	46.8	93.6	73.6	75.9	57.8	179.9	-111.0
C-1-O-5-C-5-C-4	63.6	61.7	63.8	63.1	66.7	65.0	66.4	65.0	62.1
O-5-C-5-C-4-C-3	-47.1	-52.8	-47.5	-54.0	-53.1	-54.0	-56.7	-53.6	-52.8
C-5-C-4-C-3-C-2	41.3	51.1	41.6	51.6	43.3	48.3	52.0	48.2	50.1
O-5-C-5-C-6-O-6	59.7	58.7	59.8	63.3	51.3	68.7	59.5	67.4	60.6
HO-6-O-6-C-6-C-5	-60.8	-52.6	-60.9	-57.7	-91.3	-75.4	-81.4	-76.6	-54.0

**Table 5.** B3LYP/6-311++G\*\* geometry-optimized energies (kcal/mol) and analytical Hessian-derived thermodynamic parameters for the *gg* form of the  $\alpha$ -D-glucopyranose pentahydrate

	$\alpha$ - <i>gg</i> Conformations						
	$\alpha$ - <i>gg</i> -I	$\alpha$ - <i>gg</i> -II	$\alpha$ - <i>gg</i> -III	$\alpha$ - <i>gg</i> -IV	$\alpha$ - <i>gg</i> -V	$\alpha$ - <i>gg</i> -VI	$\alpha$ - <i>gg</i> -VII
<i>E</i>	-671,295.606	-671,289.157	-671,291.317	-671,291.539	-671,297.657	-671,298.766	-671,291.699
$\Delta E$	3.995	10.444	8.284	8.063	1.944	0.835	7.902
ZPVE	203.254	202.447	202.494	202.949	202.993	203.632	202.513
$\Delta E$ ( <i>E</i> + ZPVE)	3.567	9.209	7.096	7.329	1.255	0.785	6.733
<i>E</i> glucose(st) <sup>a</sup>	-431,350.628	-431,347.420	-431,348.908	-431,344.770	-431,352.242	-431,351.768	-431,348.786
$\Delta E$ (st - vac)glucose	2.724	5.931	4.443	8.581	1.109	1.583	4.565
<i>E</i> 5-waters(st)	-239,914.466	-239,903.873	-239,905.364	-239,907.602	-239,919.709	-239,917.649	-239,908.855
$\Delta E$ (st - vac)water	-22.171	-11.678	-13.069	-15.307	-27.414	-25.354	-16.560
$\Delta E$ (total <i>E</i> - st mols)	-30.512	-37.864	-37.045	-39.167	-25.706	-29.349	-34.058
Enthalpy ( <i>H</i> )	220.084	219.751	219.289	219.960	220.007	220.307	219.298
<i>S</i> (cal/mol K)	173.293	177.331	174.891	173.817	177.897	173.359	174.434
<i>E</i> (Hyd. Bond Ave.)	-6.102	-7.573	-7.409	-7.833	-5.141	-5.870	-6.812
<i>E</i> ( $\Delta E$ /# Hyd. Bonds)	-5.085	-5.409	-7.409	-5.595	-8.569	-7.337	-4.865
$\Delta G_{298}^{\circ}$	2.957	7.869	6.149	6.734	0.990	0.000	5.738

See legends in Table 1.

<sup>a</sup> *E* (vac) $\alpha$ -*gg* glucose = -431,353.351 kcal/mol, *E* (vac)water = -47,978.459 kcal/mol  $\times$  5-waters = -239,892.295 kcal/mol.

C-2-O-2 bond length relative to that in  $\alpha$ -*gt*-I is also found, again as a result of the different hydrogen-bonding network and a change in the dihedral angle at the 3-position.

Configuration,  $\alpha$ -*gt*-III, shown in Figure 1, has some similarity to the two previous configurations, with the water bridge from the 1-hydroxyl beneath the 6-hydroxyl with hydrogen bonding around the molecule through the 6-, 4-, 3-, and 2-positions and finally back to the 1-hydroxyl position. With only two water molecules bridging below the glucose molecule between the

1-hydroxyl and 4-hydroxyl positions (instead of three waters as found in  $\alpha$ -*gt*-I), some stability of the hydrogen-bond network is lost. Accordingly, the energy of configuration  $\alpha$ -*gt*-III is  $\sim$ 6.7 kcal/mol higher than that of  $\alpha$ -*gt*-I. It is apparent from Figure 1 that the hydrogen-bond length from 1-hydroxyl to the water oxygen is longer in this configuration than that found in  $\alpha$ -*gt*-I or  $\alpha$ -*gt*-II (1.82 vs 1.74 Å). This implies that this is a weaker hydrogen bond and is a result of back donation from O-1 to the water molecule (1.78 Å) interacting with the 2-position (2.01 Å). All of the intermolecular

**Table 6.** Selected B3LYP/6-311++G\*\* optimized internal coordinates for the *gg* form of the  $\alpha$ -D-glucopyranose pentahydrates

	$\alpha$ - <i>gg</i> Conformations						
	$\alpha$ - <i>gg</i> -I	$\alpha$ - <i>gg</i> -II	$\alpha$ - <i>gg</i> -III	$\alpha$ - <i>gg</i> -IV	$\alpha$ - <i>gg</i> -V	$\alpha$ - <i>gg</i> -VI	$\alpha$ - <i>gg</i> -VII
<i>Bond lengths</i> ( $\text{\AA}$ )							
O-5-C-5	1.440	1.455	1.442	1.452	1.436	1.443	1.437
C-1-O-5	1.415	1.419	1.436	1.430	1.421	1.434	1.432
O-1-C-1	1.413	1.422	1.391	1.411	1.400	1.396	1.390
C-6-C-5	1.525	1.524	1.522	1.523	1.523	1.524	1.524
C-3-C-4	1.534	1.537	1.529	1.522	1.530	1.523	1.530
HO-1-O-1	0.963	0.975	0.984	0.985	0.982	0.982	0.986
<i>Bond angle</i> (deg)							
C-1-O-5-C-5	115.3	116.1	115.0	115.8	115.7	116.6	115.1
O-1-C-1-O-5	112.1	111.2	112.8	111.6	112.9	112.7	113.0
HO-1-O-1-C-1	109.0	107.3	109.0	109.3	107.6	108.2	108.6
O-5-C-5-C-4	111.2	112.8	110.0	111.9	109.5	109.5	109.4
O-5-C-5-C-6	105.5	105.2	108.6	105.7	106.4	106.9	108.2
HO-6-O-6-C-6	107.2	107.4	108.2	108.0	108.3	109.6	109.1
C-1-C-2-C-3	110.8	109.9	111.7	109.9	110.8	110.9	111.7
<i>Dihedral angle</i> (deg)							
HO-1-O-1-C-1-O-5	71.6	59.7	83.4	77.1	71.0	79.1	75.5
HO-2-O-2-C-2-C-1	-68.6	-69.6	-40.8	-65.0	-39.6	-39.9	-40.2
C-1-O-5-C-5-C-4	57.1	51.5	61.6	53.9	60.6	58.6	63.5
O-5-C-5-C-4-C-3	-50.6	-48.6	-58.9	-50.4	-58.2	-57.0	-58.9
C-5-C-4-C-3-C-2	48.9	52.2	56.2	53.0	56.1	56.9	55.1
O-5-C-5-C-6-O-6	-57.8	-58.2	-70.2	-58.8	-53.6	-58.1	-59.4
HO-6-O-6-C-6-C-5	56.7	54.2	-87.3	51.0	66.1	74.2	-83.3

**Table 7.** B3LYP/6-311++G\*\* geometry-optimized energies (kcal/mol) and analytical Hessian-derived thermodynamic parameters for the *gg* form of  $\beta$ -D-glucopyranose pentahydrates

	$\beta$ - <i>gg</i> Conformations							
	$\beta$ - <i>gg</i> -I	$\beta$ - <i>gg</i> -II	$\beta$ - <i>gg</i> -III	$\beta$ - <i>gg</i> -IV	$\beta$ - <i>gg</i> -V	$\beta$ - <i>gg</i> -VI	$\beta$ - <i>gg</i> -VII	$\beta$ - <i>gg</i> -VIII
<i>E</i>	-671,289.836	-671,289.547	-671,290.311	-671,291.169	-671,293.624	-671,295.090	-671,295.720	-671,298.252
$\Delta E$	9.765	10.054	9.290	8.432	5.977	4.511	3.881	1.349
ZPVE	202.100	202.760	202.896	203.053	202.213	203.202	203.095	203.893
$\Delta E$ ( <i>E</i> + ZPVE)	8.183	9.132	8.504	7.803	4.508	4.031	3.294	1.560
<i>E</i> glucose(st) <sup>a</sup>	-431,349.503	-431,342.978	-431,345.236	-431,344.875	-431,344.454	-431,344.774	-431,340.943	-431,341.465
$\Delta E$ (st - vac)glucose	2.974	9.499	7.241	7.602	8.023	7.703	11.534	11.012
<i>E</i> 5-waters(st)	-239,904.239	-239,905.538	-239,902.454	-239,909.244	-239,922.355	-239,919.487	-239,913.255	-239,919.908
$\Delta E$ (st - vac)water	-11.944	-13.243	-10.159	-16.949	-30.060	-27.192	-20.960	-27.613
$\Delta E$ (total <i>E</i> - st mols)	-36.093	-41.031	-42.621	-37.050	-26.815	-30.829	-41.522	-36.879
Enthalpy ( <i>H</i> )	219.669	219.883	219.807	219.844	217.679	219.917	219.881	220.082
<i>S</i> (cal/mol K)	182.295	174.803	172.598	171.556	161.218	172.720	174.473	166.327
<i>E</i> (Hyd. bond Ave.)	-7.219	-8.426	-8.484	-9.410	-5.363	-8.166	-8.304	-7.376
<i>E</i> ( $\Delta E$ /# Hyd. bonds)	-7.219	-6.019	-6.060	-7.841	-8.938	-8.166	-6.920	-9.220
$\Delta G_{298}^{\circ}$	5.629	8.365	8.182	7.671	6.132	3.476	2.288	2.385

See legends in Table 1.

<sup>a</sup> *E* (vac) $\beta$ -*gg* glucose = -431,352.477 kcal/mol, *E* (vac)water = -47,978.459 kcal/mol  $\times$  5-waters = -239,892.295 kcal/mol.

hydrogen bonds are perturbed by the presence of water molecules, resulting in HO-*n*...O-(*n* - 1) distances in the 2.6–2.8 Å range (*n* = 2, 3, 4). This change in hydrogen bonding results in significant rotations of the hydroxyl groups hydrogen atoms (relative to the positions in isolated glucose); accordingly, the glucose stress energy is larger in this configuration than in  $\alpha$ -*gt*-I or  $\alpha$ -*gt*-II.

Configuration  $\alpha$ -*gt*-IV is shown in Figure 1. This configuration has only one water molecule interacting with the 1-hydroxyl position, and the other four waters

are located around the 2-, 3- and 4-hydroxyl groups. The configuration is compact, and the water–water interaction energy given in Table 1 is considerably larger than that found in the previous three configurations. A short hydrogen bond is found between HO-3 and O(water) (~1.69 Å), a result of this water having two donor interactions and one acceptor interaction. The HO-1...O(water) distance is 1.89 Å, implying a weaker interaction than found in  $\alpha$ -*gt*-I and a result of the water donating to the O-6 atom. Because of the direction of

**Table 8.** Selected B3LYP/6-311++G\*\* optimized internal coordinates for the *gg* form of the  $\beta$ -D-glucopyranose pentahydrates

	$\beta$ - <i>gg</i> Conformations							
	$\beta$ - <i>gg</i> -I	$\beta$ - <i>gg</i> -II	$\beta$ - <i>gg</i> -III	$\beta$ - <i>gg</i> -IV	$\beta$ - <i>gg</i> -V	$\beta$ - <i>gg</i> -VI	$\beta$ - <i>gg</i> -VII	$\beta$ - <i>gg</i> -VIII
<i>Bond lengths (Å)</i>								
O-5-C-5	1.436	1.447	1.439	1.437	1.432	1.440	1.427	1.429
C-1-O-5	1.426	1.412	1.399	1.424	1.411	1.434	1.435	1.419
O-1-C-1	1.408	1.413	1.411	1.398	1.409	1.391	1.386	1.406
C-6-C-5	1.525	1.522	1.529	1.526	1.528	1.528	1.519	1.517
C-3-C-4	1.528	1.535	1.533	1.531	1.523	1.527	1.530	1.523
HO-1-O-1	0.964	0.966	0.979	0.982	0.979	0.978	0.975	0.980
<i>Bond angle (deg)</i>								
C-1-O-5-C-5	114.1	112.2	114.5	113.5	116.7	114.6	114.6	113.8
O-1-C-1-O-5	107.1	105.9	106.0	105.1	103.0	106.4	106.8	105.0
HO-1-O-1-C-1	108.7	106.6	107.8	111.3	111.3	110.9	111.1	110.9
O-5-C-5-C-4	110.7	111.7	113.0	111.3	110.1	109.4	111.9	110.5
O-5-C-5-C-6	105.8	108.2	105.9	107.3	105.3	108.0	107.8	107.9
HO-6-O-6-C-6	107.0	108.7	110.4	108.2	107.2	108.6	108.9	109.2
C-1-C-2-C-3	108.2	108.2	108.1	109.4	109.6	109.2	109.4	108.1
<i>Dihedral angle (deg)</i>								
HO-1-O-1-C-1-O-5	-75.5	-174.2	-158.9	-160.9	162.8	113.9	113.3	145.1
HO-2-O-2-C-2-C-1	94.4	104.0	103.2	85.5	70.4	75.7	80.2	81.5
C-1-O-5-C-5-C-4	59.6	59.3	53.8	61.6	57.8	60.8	59.2	60.0
O-5-C-5-C-4-C-3	-49.5	-48.9	-43.4	-52.1	-53.8	-53.6	-50.8	-53.5
C-5-C-4-C-3-C-2	49.2	48.5	47.0	50.7	54.6	52.9	51.2	53.7
O-5-C-5-C-6-O-6	-57.5	-66.2	-67.5	-55.0	-53.1	-60.7	-62.5	-64.8
HO-6-O-6-C-6-C-5	56.6	128.0	66.5	84.9	62.3	80.0	-156.9	-168.5

**Table 9.** B3LYP/6-311++G\*\* geometry-optimized energies (kcal/mol) and analytical Hessian-derived thermodynamic parameters for the *tg* hydroxymethyl form of  $\alpha$ - and  $\beta$ -D-glucopyranose pentahydrates

	$\alpha$ - <i>tg</i> Conformations				$\beta$ - <i>tg</i> Conformations		
	$\alpha$ - <i>tg</i> -I	$\alpha$ - <i>tg</i> -II	$\alpha$ - <i>tg</i> -III	$\alpha$ - <i>tg</i> -IV	$\beta$ - <i>tg</i> -I	$\beta$ - <i>tg</i> -II	$\beta$ - <i>tg</i> -III
<i>E</i>	-671,290.504	-671,284.891	-671,291.759	-671,290.421	-671,289.417	-671,288.061	-671,294.422
$\Delta E$	9.097	14.710	7.842	9.180	10.184	11.540	5.179
ZPVE	202.739	202.033	203.034	203.328	202.525	202.137	203.291
$\Delta E (E + \text{ZPVE}(H))$	8.154	13.061	7.194	8.826	9.027	9.995	4.788
<i>E</i> glucose(st) <sup>a</sup>	-431,346.790	-431,340.384	-431,349.521	-431,349.848	-431,348.552	-431,349.018	-431,350.697
$\Delta E (\text{st} - \text{vac})\text{glucose}$	6.581	12.987	3.850	3.523	3.791	3.325	1.646
<i>E</i> 5-waters(st)	-239,903.807	-239,906.448	-239,913.264	-239,913.415	-239,903.869	-239,899.090	-239,926.661
$\Delta E (\text{st} - \text{vac})\text{water}$	-11.512	-14.153	-20.969	-21.120	-11.574	-6.795	-34.366
$\Delta E (\text{total } E - \text{st mols})$	-39.907	-38.059	-28.974	-27.158	-36.996	-39.951	-17.064
Enthalpy ( <i>H</i> )	219.864	219.630	219.353	220.275	219.308	219.632	219.310
<i>S</i> (cal/mol K)	176.059	183.716	169.440	173.181	173.158	180.586	166.612
<i>E</i> (Hyd. bond Ave.)	-7.981	-7.612	-5.795	-5.431	-7.399	-7.990	-3.613
<i>E</i> ( $\Delta E/\#$ Hyd. bonds)	-5.701	-5.437	-4.829	-4.526	-6.166	-5.707	-6.021
$\Delta G_{298}^{\circ}$	7.014	10.112	7.221	8.366	8.410	7.876	5.358

See legends in Table 1.

<sup>a</sup> *E* (vac) $\alpha$ -*tg* glucose = -431353.371,  $\beta$ -*tg* glucose = -431,352.343 kcal/mol, *E* (vac)water = -479,78.459 kcal/mol  $\times$  5-waters = -239,892.295 kcal/mol.

the H(water)··O-2 hydrogen bond (2.14 Å), the dihedral angle around the C-2-O-2 bond remains at  $\sim -37^\circ$  and a short strong interaction between HO-2 and O-1 (2.11 Å) remains. On the other hand, the dihedral angles (see Table 2) at the 3- and 4-hydroxyl positions are perturbed by  $\sim 20^\circ$  from the vacuum case, indicating the ability of the four water molecules to break the intramolecular interaction network in glucose.

The configuration  $\alpha$ -*gt*-V is shown in Figure 1. This complex was studied to attempt to cluster water molecules around the 1- and 2-positions and resulted in one water molecule being hydrogen bonded only to other water molecules. As can be seen in Table 1, the water-water interaction energy is large. Of interest is the value of the HO-1-O-1-C-1-O-5 dihedral angle ( $\sim +109^\circ$ ) relative to a  $67^\circ$  value for the vacuum case. This nearly  $40^\circ$  change is significant because the total electronic energy



**Table 10.** Selected B3LYP/6-311++G\*\* optimized internal coordinates for the *tg* form of the  $\alpha$ - and  $\beta$ -D-glucopyranose pentahydrates

	$\alpha$ Anomers				$\beta$ Anomers		
	$\alpha$ - <i>tg</i> -I	$\alpha$ - <i>tg</i> -II	$\alpha$ - <i>tg</i> -III	$\alpha$ - <i>tg</i> -IV	$\beta$ - <i>tg</i> -I	$\beta$ - <i>tg</i> -II	$\beta$ - <i>tg</i> -III
<i>Bond lengths (Å)</i>							
O-5-C-5	1.446	1.437	1.456	1.442	1.440	1.436	1.439
C-1-O-5	1.420	1.398	1.414	1.433	1.420	1.441	1.416
O-1-C-1	1.423	1.427	1.394	1.409	1.388	1.394	1.381
C-6-C-5	1.530	1.530	1.543	1.523	1.532	1.533	1.554
C-3-C-4	1.535	1.534	1.565	1.530	1.549	1.526	1.538
HO-1-O-1	0.976	0.977	0.964	0.974	0.962	0.977	0.979
<i>Bond angle (deg)</i>							
C-1-O-5-C-5	115.0	115.5	116.1	115.3	114.0	114.1	114.0
O-1-C-1-O-5	111.2	108.5	108.2	111.4	104.1	107.5	104.7
HO-1-O-1-C-1	107.1	111.4	111.1	107.4	106.3	108.2	104.8
O-5-C-5-C-4	110.8	109.1	111.6	108.3	110.7	109.8	110.2
O-5-C-5-C-6	107.1	106.5	109.0	106.7	108.4	106.7	108.6
HO-6-O-6-C-6	106.4	107.1	108.5	107.8	107.7	107.1	108.1
C-1-C-2-C-3	110.1	111.2	111.1	109.6	109.5	109.4	108.6
<i>Dihedral angle (deg)</i>							
HO-1-O-1-C-1-O-5	59.4	−171.5	31.9	63.6	−58.0	−62.7	45.1
HO-2-O-2-C-2-C-1	−68.5	−70.0	−58.4	−66.6	66.4	94.5	60.6
C-1-O-5-C-5-C-4	56.9	58.7	56.8	56.9	59.9	61.1	60.1
O-5-C-5-C-4-C-3	−55.7	−56.9	−53.4	−57.8	−53.0	−54.4	−54.6
C-5-C-4-C-3-C-2	56.1	54.2	50.4	57.5	51.1	52.9	53.9
O-5-C-5-C-6-O-6	162.1	165.9	170.4	169.7	174.5	166.8	172.7
HO-6-O-6-C-6-C-5	47.5	48.2	47.8	58.4	47.8	47.8	45.9

of this configuration is only a few kcal/mol higher than the lowest energy  $\alpha$ -configuration. The dihedral angle HO-2-O-2-C-2-C-1 (−63.9°) has also become more negative relative to the vacuum state by  $\sim 20^\circ$ , breaking the close hydrogen bond between the HO-2 and O-1 atoms (now 2.64 Å apart). The HO-2-O-2-C-2 bond angle is also enlarged significantly, from a value of  $\sim 106^\circ$  in  $\alpha$ -*gt*-IV to  $\sim 113^\circ$  in  $\alpha$ -*gt*-V. This is a result of two short (1.73 and 1.74 Å) hydrogen bonds (donor and acceptor) formed to two water molecules (see Fig. 1).

The configuration  $\alpha$ -*gt*-VI is shown in Figure 1. The 1-hydroxyl group hydrogen bonds to two water molecules acting as both donor and acceptor, the result being fairly long hydrogen bonds (1.95 and 1.86 Å). The 2-position also has both donor and acceptor interactions, as does the 3-position. The HO-2...O-1 hydrogen bond is now completely broken, as both the 1- and 2-hydroxyl groups are donors to the same water oxygen atom. The concomitant structural changes result in an enormous increase in the glucose stress energy; this is why  $\alpha$ -*gt*-VI is considerably higher in energy than  $\alpha$ -*gt*-I. The 4-hydroxyl group only acts as a donor to a water molecule and (more weakly) to the 3-OH (2.76 Å).

The  $\alpha$ -*gt* geometries in Table 2 are a subset of all the internal coordinates for the six configurations of water around the *gt* conformation. However, this subset is sufficient to show the major changes, relative to the in vacuo glucose *gt* conformation, upon addition of five water molecules. The bond lengths and bond angles show only the expected small deviations as different con-

figurations of water molecules are examined. However, the soft variables, the dihedral angles, are significantly modified by the different water configurations. For example, the HO-1-O-1-C-1-C-5 dihedral angle varies between  $\sim 13^\circ$  and  $-140^\circ$  in conformers  $\alpha$ -*gt*-III and  $\alpha$ -*gt*-VI, and  $+109^\circ$  in conformer  $\alpha$ -*gt*-V. The fact that these variances are important is seen in the ring dihedral angle, C-1-O-5-C-5-C-4, with a value of  $49.4^\circ$  in  $\alpha$ -*gt*-III and  $69.8^\circ$  in  $\alpha$ -*gt*-VI. A  $20^\circ$  change in ring conformation accompanies a significant change in the dihedral angle at the 1-position. A large variance between configurations was also observed in the O-5-C-5-C-4-C-3 dihedral angle. The hydroxymethyl group variance in the dihedral angle for this set of data is  $\sim 19^\circ$  maximum between conformers IV and V.

### 3.2. $\beta$ -*gt* Conformations

The  $\beta$  configuration denoted  $\beta$ -*gt*-I is shown in Figure 2. The water configuration of this structure is similar to that found in  $\alpha$ -*gt*-I. The water molecule in the 1-position is hydrogen bonded (1.93 Å) as an acceptor to the OH-1 as well as hydrogen bonded to a second water molecule (1.82 Å) as a hydrogen donor. The water molecules at the 3- and 4-positions are fairly close to the same configurations found for the monohydrates at those positions.<sup>1</sup> The hydrogen bond geometries, shown in Figure 2, have glucose to water hydrogen-bond distances varying from two short 1.81 Å bonds for both the HO-3...O water and HO-4...O water, to 2.03 Å

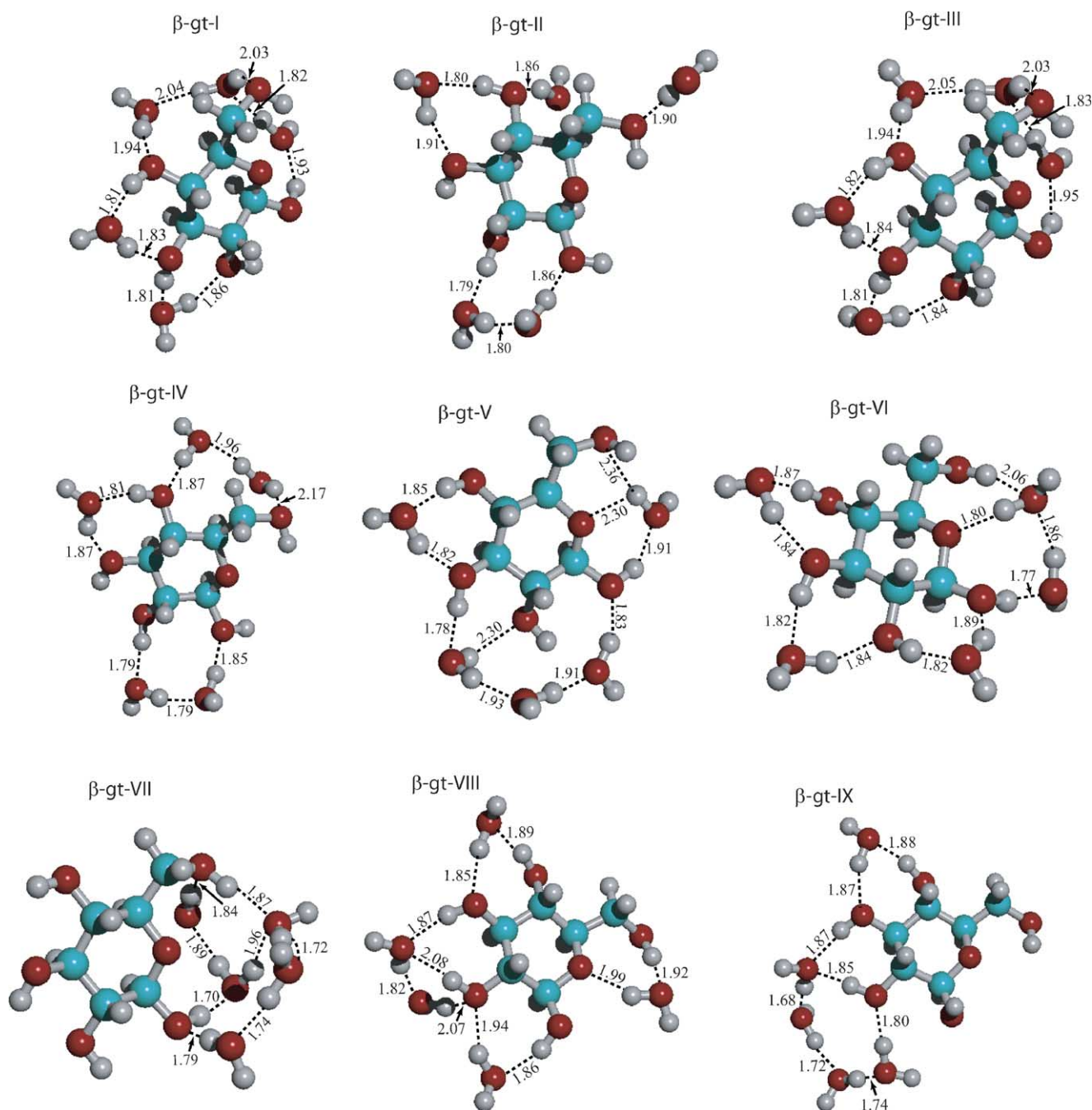


**Figure 2.** Hydrogen-bonding configurations of water molecules about  $\beta$ -gt.

for O-6 $\cdots$ H water. In Table 3, energies for the  $\beta$ -gt configurations are presented, and conformation  $\beta$ -gt-VII is seen to be the lowest energy configuration found. It is clear from Table 3 that significant differences in the equilibrium structures exist, depending upon where the five water molecules are placed. As with the  $\alpha$ -gt structures, we observed major changes in dihedral angles that are directly related to the positions of the water molecules showing considerable variances (up to 50°) in dihedral angle between configurations even though each started from the same sugar conformation (Table 4).

In the  $\beta$ -gt-I case, the HO-2-O-2-C-2-C-1 dihedral angle is small ( $\sim 43^\circ$ , which is  $\sim 20^\circ$  smaller than the value in isolated glucose), due to interactions with a water molecule beneath the 3-position.

In the  $\beta$ -gt-II configuration, the 1- and 2-hydroxyl groups are connected by a chain of two water molecules; this accounts for the HO-2-O-2-C-2-C-1 dihedral angle difference between this complex ( $\sim 95^\circ$ ) and the  $\beta$ -gt-I configuration ( $\sim 43^\circ$ ). This particular configuration of water molecules was not found in the  $\alpha$ -gt series, as the proximity of the 1- and 2-hydroxyl groups in  $\alpha$ -glucose

would cause this arrangement to have significant ring strain. The two water chain has the effect of expanding the HO-2...O-1 distance to 2.97 Å, and making the OH bonds on hydroxyl groups #1 and #2 nearly perpendicular to one another. Accordingly, the intermolecular interaction between these groups is likely very small, thus decreasing the ring polarization. In addition, two of the water molecules participate in only one hydrogen bond each. These two facts explain why the  $\beta$ -*gt*-II configuration is the least stable of all of the  $\beta$ -*gt* structures. Further, the other water molecules are spread out around the glucose molecule resulting in a water–water interaction energy, which is among the smallest of all the pentahydrates studied. That there are two single-hydrogen bonded waters also explains the relatively high entropy of this configuration (see Table 3).

The configuration around  $\beta$ -*gt*-III, shown in Figure 2, is almost identical to that found in  $\beta$ -*gt*-I. The difference is in the interaction of the lone pair electrons of the water molecule at the 2- and 3-positions, which direct the tilt of the water molecule differently in the two configurations. The subtle effect that this has on the internal coordinates of the two configurations is given in Table 4 where small changes in dihedral angles arise just from this small deviation in this water molecule. For example, the dihedral angle, HO-2–O-2–C-2–C-1, changes by 3.7° because of this subtle orientation change in a water molecule. As expected, the total interaction energies and stress energies are very similar for these two structures.

The configuration  $\beta$ -*gt*-IV, shown in Figure 2, is similar to  $\beta$ -*gt*-II and like  $\beta$ -*gt*-II is also not of low energy. The main differences between these structures are that  $\beta$ -*gt*-IV has a 2-water bridge between the 4-hydroxyl and hydroxymethyl oxygen, whereas in structure  $\beta$ -*gt*-II, these two water molecules are not hydrogen bonded to each other. Because the glucose molecule is in the  $\beta$  anomeric form, the hydrogen bonds in the chain of water molecules can bridge between the 1- and 4-hydroxyl groups. From the region of the 4-hydroxyl group counterclockwise back to the 1-hydroxyl group there is also a break in the network, with no water molecule taking up the position between the 2- and 3-hydroxyl groups. Consequently, this complex is ~4 kcal/mol higher in energy than  $\alpha$ -*gt*-I, even though in the vacuum glucose case the  $\alpha$ -*gt* and  $\beta$ -*gt* conformers were nearly identical in energy.<sup>1</sup>

If we continue this train of thought and apply it to configuration  $\beta$ -*gt*-V (see Fig. 2), the break in the ring of hydrogen bonds is again apparent under the 6-hydroxyl position. With four water molecules around the 1-, 2-, and 3-hydroxyl positions, the energy is somewhat lower than configuration  $\beta$ -*gt*-IV but not as low as those configurations that have a more complete network of hydrogen bonds around the glucose molecule, or have a cluster of water molecules near the 1-hydroxyl as in  $\beta$ -*gt*-VII (see Fig. 2). The unusual dihedral angle in  $\beta$ -

*gt*-V is that of HO-6–O-6–C-6–C-5, which has become larger (Table 4) relative to the other configurations by more than 30°. This dihedral angle change is a result of a water forming three hydrogen bonds, H(water)–O-6 (2.36 Å) and H(water)··O-5 (2.30 Å) as well as O(water)··HO-1 (1.91 Å). Apparently this water molecule holds the HO-1–O-1–C-1–O-5 dihedral angle at ~60°, and the stress is applied to the 6-hydroxyl, forcing the dihedral angle change just described.

The configuration  $\beta$ -*gt*-VI (Fig. 2) has a network of hydrogen bonds in a clockwise direction from the 1-hydroxyl through to the 4-hydroxyl, with the 6-hydroxyl locked into place by interactions from the two water chain that extends to the 1-hydroxyl group. This configuration is unusual in that one water molecule has a close hydrogen bond to O-5 (1.80 Å). Typically, this interaction is not found in the *gt* series since the hydroxymethyl group usually prevents such close contact to the O-5 oxygen. The average hydrogen-bond energy (–9.1 kcal/mol) is the largest of all the  $\beta$ -*gt* configurations studied, a result of the large number (9) of glucose–water hydrogen bonds formed.

Configuration  $\beta$ -*gt*-VII (Fig. 2) clusters the water molecules around the 1-hydroxyl and the 6-hydroxyl groups. This configuration has the lowest electronic and ZPVE corrected energy of all the glucose pentahydrates studied, due to a large water–water interaction energy (~25.7 kcal/mol) and low glucose stress energy (2.2 kcal/mol); however, this configuration does not have the lowest free energy ( $\Delta G \sim 0.5$  kcal/mol). This is because both the hydroxymethyl group and two of the water molecules are restricted in their motions, resulting in a lower-than-average entropy. The most obvious internal geometry change relative to the other configurations is at the dihedral angle, HO-6–O-6–C-6–C-5, which becomes ~20° more negative than the standard –60° value. Interestingly, the dihedral angle HO-1–O-1–C-1–O-5, has not changed significantly from the vacuum glucose value, even though the water molecules are clustered around the 1-position.

$\beta$ -*gt*-VIII has a water molecule located on every glucose hydroxyl group, either as a donor or acceptor or both. The 2- and 3-hydroxyl hydrogens point toward one water's oxygen (2.08 and 1.87 Å, respectively). The 1-hydroxyl dihedral angle, HO-1–O-1–C-1–O-5, has rotated to ~161°, and the dihedral angle of HO-2–O-2–C-2–C-1 has also rotated significantly, both becoming clockwise while the 3- and 4-hydroxyl groups retain the counterclockwise configuration. This complex has nine glucose–water hydrogen bonds and only one water–water hydrogen bond, resulting in a large glucose stress energy and large glucose–water interaction energy. The glucose–water hydrogen bonds do not completely compensate for the glucose stress and the small water–water interaction energy, and this is one of the least stable structures found.

Configuration  $\beta$ -*gt*-IX has no water molecules near the O-5, 1-, or 6-hydroxyl positions. Two water molecules are not interacting with glucose, only hydrogen bonding to other waters. Because of the water molecule interacting with both O-1 and O-2, the HO-1–O-1–C-1–O-5 dihedral angle is rotated to  $+60^\circ$  (from  $-67^\circ$  in the vacuum case<sup>1</sup>), while the HO-2–O-2–C-2–C-1 dihedral angle is now  $-111^\circ$ , allowing both the 2- and 3-hydroxyl hydrogens to point to the same water's oxygen (1.85 and 1.87 Å).

### 3.3. $\alpha$ -*gg* Conformations

One feature of the *gg* conformation that sets it apart from the *gt* conformation is the ability of water molecules to approach the O-5 atom of the sugar ring, since

the hydroxymethyl group is out of the way. This was not found routinely with the *gt* configurations and must be considered when looking at the differences between the *gt* and *gg* hydrates.

Configuration  $\alpha$ -*gg*-I (Fig. 3) is of interest because the water molecules are all placed around the 2-, 3-, and 4-positions, with no waters near the 1- or 6-positions. Note that the energy is relatively low ( $\Delta E \sim 4$  kcal/mol), but this configuration will have no bearing on the hydroxymethyl rotamer population since it has no water molecules near the 6-position. One water molecule is not in contact with the glucose molecule, hydrogen bonding (1.75 and 1.74 Å) only to other water molecules. It is of interest that the dihedral angle, HO-2–O-2–C-2–C-1, did not change significantly from the vacuum case, even though one of the two water molecules

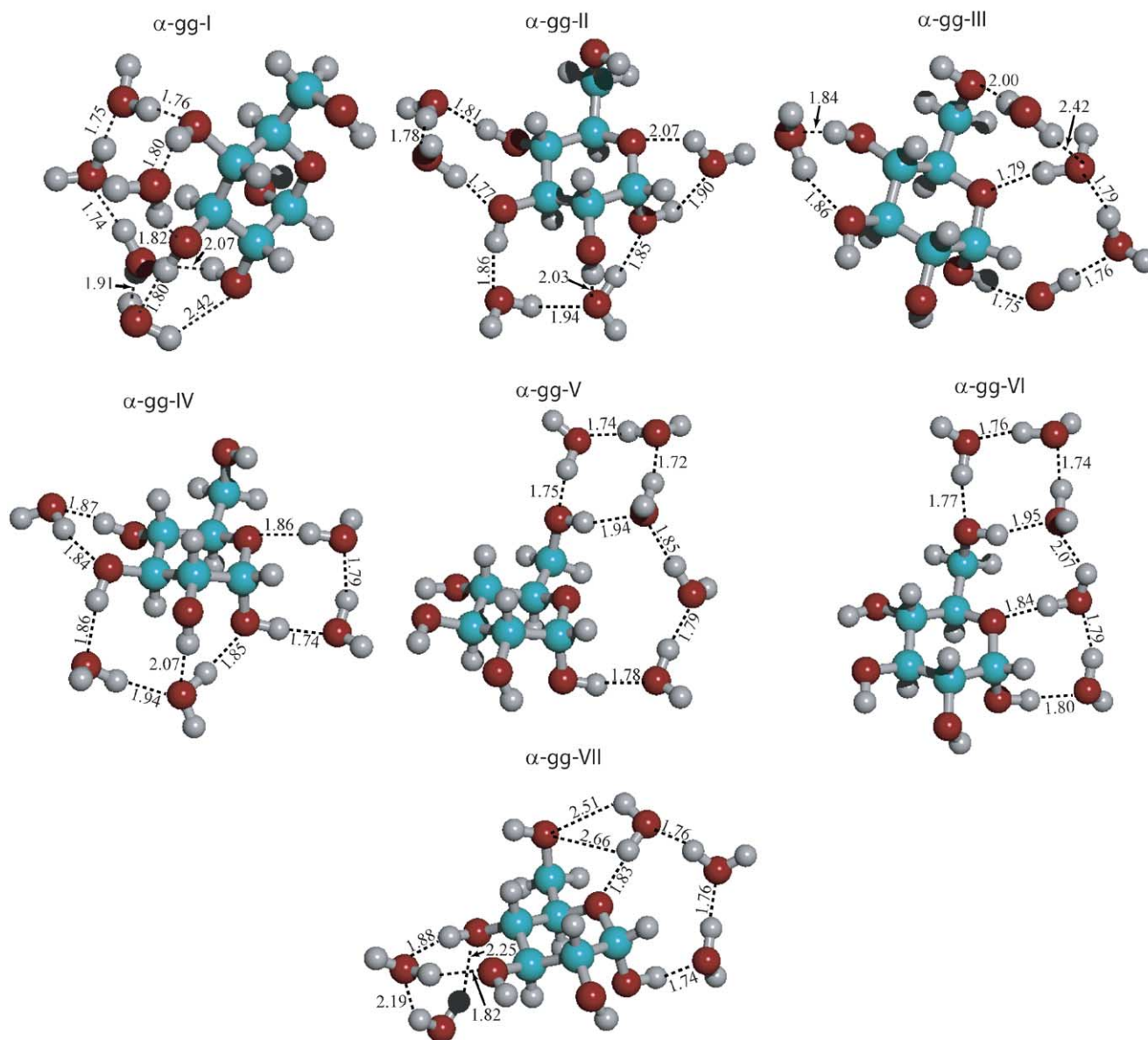


Figure 3. Hydrogen-bonding configurations of water molecules about  $\alpha$ -*gg*.



interacting with this hydroxyl group has a long hydrogen-bond length (2.42 Å) and is a fairly weak interaction. The 3- and 4-hydroxyl groups act as both donor and acceptor to water molecules.

Configuration  $\alpha$ -gg-II (Fig. 3) has a water molecule interacting at the 1-position (1.90 Å) and hydrogen bonding (2.07 Å) to the O-5 oxygen atom. The other water molecules (both donor and acceptor) are spaced around the 2-, 3-, and 4-positions, with the 6-hydroxyl again not interacting directly with a water molecule. Hydroxyl groups at the 1-, 2-, 3-, and 4-positions all are donors, and the 1- and 3-hydroxyls are also acceptors from water molecules. Comparing  $\alpha$ -gg-I with  $\alpha$ -gg-II, we see that the latter has fewer water–water hydrogen bonds and more glucose–water hydrogen bonds. The increase in stability due to the glucose–water interactions does not fully compensate for the lower glucose stress and stronger water–water interactions in  $\alpha$ -gg-I, so  $\alpha$ -gg-II is  $\sim 7$  kcal/mol less stable than  $\alpha$ -gg-I.

Configuration  $\alpha$ -gg-III (Fig. 3) has water interacting as an acceptor at the 1- and 4-positions, and donor waters at the 3- and 6-positions, and with the O-5 oxygen atom (1.79 Å). In this, as well as other gg clusters, we see a chain of water molecules originating from the 1-position and ending at the 6-position (cf. the 1 $\rightarrow$ 6 $\rightarrow$ 4 chains present in the gt structures). This results in a restriction of the hydroxymethyl orientation in these structures. This structure has the longest such chain, that is, four water molecules, and one of the water molecules participates in the chain as a double acceptor; the end result is that there is less polarization of the water molecules in the chain, and the water–water interaction energy per water–water hydrogen bond ( $-4.32$  kcal/mol) is lower in this structure than in any other studied. Water does influence the hydroxymethyl group conformation in this configuration.

$\alpha$ -gg-IV Configuration (Fig. 3) is similar to  $\alpha$ -gg-II, except that in  $\alpha$ -gg-IV the HO-1 $\cdots$ O-5 bridge consists of two water molecules, while the HO-4 $\cdots$ O-3 bridge consists of one water molecule (the reverse is true in  $\alpha$ -gg-II).

The configurations denoted  $\alpha$ -gg-V and  $\alpha$ -gg-VI (Fig. 3) are nearly identical to one another, except that in  $\alpha$ -gg-VI there is a water-to-O-5 hydrogen bond. As one would expect, this means that  $\alpha$ -gg-V has stronger water–water hydrogen bonding and weaker glucose–water hydrogen bonding. In addition, the glucose stress energy is slightly higher in configuration VI. The net result is that  $\alpha$ -gg-V is slightly more stable than  $\alpha$ -gg-VI, both structures being of low energy, only 1–2 kcal/mol higher in energy than the lowest energy structure found.

Configuration  $\alpha$ -gg-VII (Fig. 3) has several unusual features: One water molecule has two hydrogen atoms interaction with the same oxygen atom (O-6) in a bifurcated arrangement, while one of these hydrogen atoms is also hydrogen bonded to O-5. In addition, the two water

molecules on the other side of the glucose molecule are in unusual hydrogen-bonding arrangements, with one acting as a double donor and the other acting as a single donor, double acceptor. The resulting structure has a  $\Delta E$  value of  $\sim 8$  kcal/mol, which is relatively high.

### 3.4. $\beta$ -gg Conformations

The  $\beta$ -gg conformers are of fairly high energy, the exception being  $\beta$ -gg-VIII, which is only  $\sim 1.3$  kcal/mol higher in energy than the lowest energy configuration found.

Configuration  $\beta$ -gg-I (Fig. 4) has two water molecules near the anomeric hydroxyl and 2-position hydroxyl with three water molecules interacting at the 3- and 4-hydroxyl positions. The 2-hydroxyl dihedral is perturbed leading to an increase in the HO-2 $\cdots$ O-1 hydrogen-bond length. No water molecules interact with the hydroxymethyl group.

Configuration  $\beta$ -gg-II (Fig. 4) is the least stable of the  $\beta$ -gg clusters, despite the stronger-than-average glucose–water interactions. The complex is stabilized by the network of water molecules connecting the 1- and 6-hydroxyl groups, but the water molecules in that network are highly stressed, giving an interaction energy of only  $\sim 4.4$  kcal/mol per hydrogen bond. There are four water molecules on the 6-hydroxymethyl, O-5, 1-, and 2-hydroxyl groups, and one molecule interacting between the 3- and 4-hydroxyl region. HO-1 has been rotated until it is now turned toward the 2-position. The 1- and 2-hydroxyl groups are connected by a chain of two water molecules, one donating to the O-1 (1.98 Å) and the HO-2 donating (1.80 Å) to the second water.

Configuration  $\beta$ -gg-III (Fig. 4) has four water molecules around the hydroxymethyl, O-5, 1-hydroxyl (1.72 Å), and 2-hydroxyl (1.90 Å), with the HO-2 pointing up toward a water (1.81 Å) and away from O-1, thus breaking the ring hydrogen-bonding network. The 1-hydroxyl has rotated away from the O-5 atom and points as a donor hydrogen (1.83 Å) to the same water that donates a hydrogen to the O-2 atom. The fifth water molecule interacts at the 3- and 4-hydroxyl groups donating a proton to O-3 and acceptor to HO-4.

Configuration  $\beta$ -gg-IV (Fig. 4) also has four water molecules spaced around the O-5 (2.02 Å), HO-1, and HO-2 groups, but in a different configuration than those described above for  $\beta$ -gg-III. Again the 1-hydroxyl is pointing toward the 2-position, donating a proton (1.79 Å) to a water molecule.

Configuration  $\beta$ -gg-V (Fig. 4) clusters the water molecules around the 6-hydroxyl, 5-oxygen, and the anomeric hydroxyl, rotating the anomeric hydroxyl group to point toward a water (1.82 Å) and toward the 2-hydroxyl hydrogen. This is a major change in structure from  $\beta$ -gg-III and  $\beta$ -gg-IV creating a crab-like condition



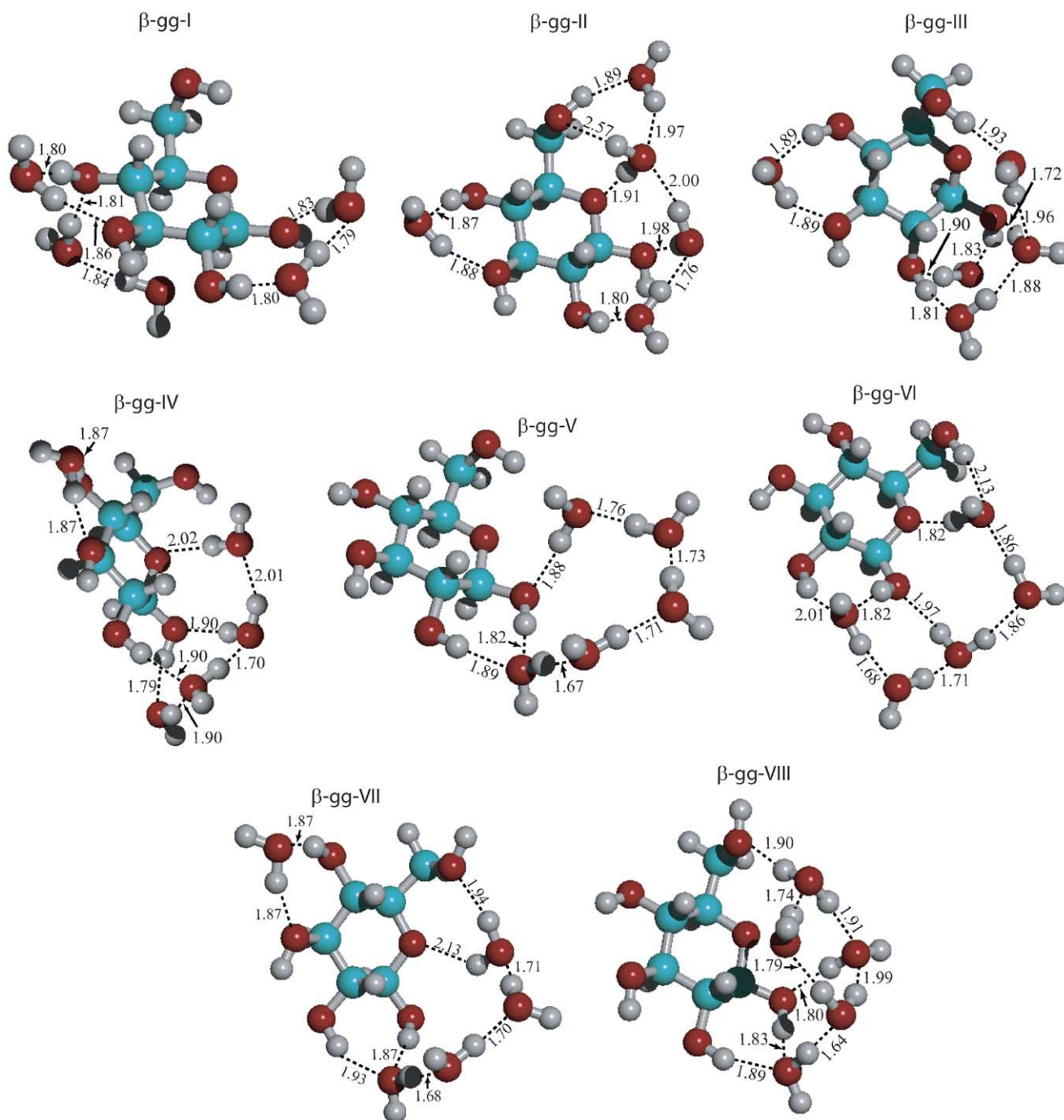


**Figure 4.** Hydrogen-bonding configurations of water molecules about  $\beta$ -gg.

between the 1- and 2-positions in which both hydroxyl groups donate protons to the water oxygen acceptor atom. Three water molecules are hydrogen bonded only to other water molecules.

Configuration  $\beta$ -gg-VI (Fig. 4) is similar to  $\beta$ -gg-V but with the 6-hydroxyl now taking part in the hydrogen-bond network. The 1- and 2-hydroxyl groups both donate to the same water molecule (2.01 and 1.82 Å), which is also hydrogen bonded to another water through a very short hydrogen bond (1.68 Å) showing

an inductive effect of the two donor interactions from the glucose.

Configuration  $\beta$ -gg-VII (Fig. 4) is again similar to  $\beta$ -gg-II and  $\beta$ -gg-VI, but with a different network of hydrogen bonds from the hydroxymethyl group to the 2-hydroxyl. This configuration is the lowest free energy  $\beta$ -gg form (see Table 7) found in this study, although the electronic energy of  $\beta$ -gg-VIII is lower.

Configuration  $\beta$ -gg-VIII (Fig. 4) also has all five water molecules around the O-5 face of the glucose molecule.

The 1- and 2-hydroxyl groups donate the same water oxygen atom, and the network includes the hydroxymethyl group linked around to the 2-hydroxyl. This configuration is the lowest energy  $\beta$ -*gg* form, due to a combination of strong water–water and glucose–water interactions.

### 3.5. $\alpha$ -*tg* Conformations

The  $\alpha$ -*tg* and  $\beta$ -*tg* configurations all have the O-5-C-5–C-6–O-6 dihedral angle near  $180^\circ$ , but because of inter-

actions with the water molecules, other exocyclic hydroxyl groups are distorted out of the normal counterclockwise configurations. The result of all the interactions is that the *tg* configurations are all relatively high in energy (see Table 9).

Configuration  $\alpha$ -*tg*-I (Fig. 5) shows that the two water molecules interacting with the 3-hydroxyl and 4-hydroxyl groups have rotated the 4-hydroxyl group out of an optimal position to point toward the water molecule partially hydrogen bonded to the 3-hydroxyl. This geometry also strains the water–water hydrogen bond,

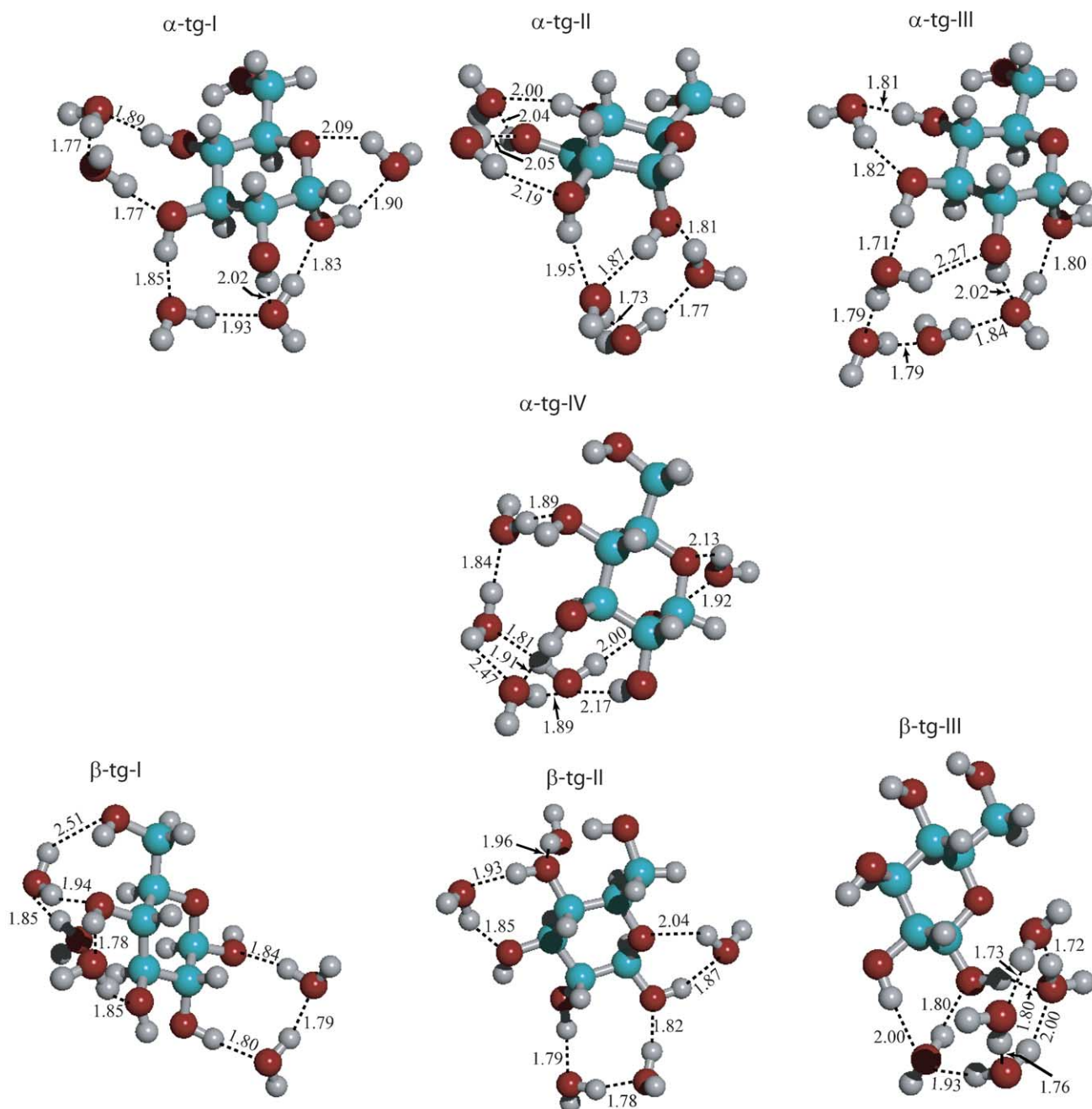


**Figure 5.** Hydrogen-bonding configurations of water molecules about  $\alpha$ -*tg* and  $\beta$ -*tg*.

resulting in weaker water–water interactions. Additionally, the 2-hydroxyl is pointed down toward the water at that position, away from the normal interaction between HO-2 and O-1.

Configuration  $\alpha$ -*tg*-II (Fig. 5) shows that the 1-hydroxyl group (HO-1–O-1–C-1–O-5 =  $-171.5^\circ$ ) is rotated away from the O-5 atom and is pointing more toward the 2-hydroxyl group, forming a crab-like donor configuration with the water molecules (1.95 and 1.87 Å) interacting at this site. This structure has the highest glucose stress energy of any studied, and the highest total energy of the *tg* clusters.

Configuration  $\alpha$ -*tg*-III (Fig. 5) shows that the water molecules are removed to some extent from the glucose molecule forming a network of water–water hydrogen bonds between the 1- and 3-positions.

Configuration  $\alpha$ -*tg*-IV (Fig. 5) has the 1-position water molecule (1.92 Å) also weakly hydrogen bonded to O-5 (2.13 Å) and waters below the 2-, 3-, and 4-positions. The total electronic energy is relatively high, again due to relatively weak glucose–water interactions.

### 3.6. $\beta$ -*tg* Conformations

Configuration  $\beta$ -*tg*-I (Fig. 5) has water molecules interacting at the 1-, 2-, 3-, and 4-positions but very little distortion of the hydroxyl dihedral angles as a result of these interactions. As with  $\beta$ -*gg*-I, there is a single hydrogen-bonded water molecule, as well as a 2-water bridge between two consecutive hydroxyl groups. Consequently, the energy of this complex is high.

Configuration  $\beta$ -*tg*-II (Fig. 5) shows distortion in the 2- and 4-hydroxyl groups; that is, the hydroxyl OH atoms have rotated out of their optimal values to create close interactions with the water molecules at the 2-position as well as the 4-position. Despite this, the glucose stress energy is not particularly high. However, the water–water interactions are weak, resulting in a complex of relatively high energy.

Configuration  $\beta$ -*tg*-III (Fig. 5) shows all five water molecules located around the 1-hydroxyl group rotating the 1-position dihedral into a  $+45^\circ$  position. The glucose stress energy for this structure is very low. Water–water interactions play the major stabilizing role for this configuration, and the total electronic energy is the lowest of all the *tg* conformations (see Table 9). The water–water energy is the most stable by far of all the different configurations.

## 4. General conclusions

One interesting observation of the *gt* pentahydrates is the formation of a string of three water molecules located below the hydroxymethyl group. This linked water string occurs in both of the  $\alpha$  anomers (see Fig. 1) and

also in a slightly expanded form in the one  $\beta$  anomer (see Fig. 2). Starting at the HO-1 position hydrogen bonded to the O(water), the H(water) then interacts with the second water molecule, which interacts with OH-6. The interaction of the last H(water) to OH-4 continues the string, and the continuation on from the HO-4 to O(water), and the further interaction of the H(water) to the OH-3, etc., finishes the ring of hydrogen bonding.

For some time we have questioned why the crystallographic C-5–C-6 bond lengths have been short relative to the calculated values. To address this question using results collected here, we report the C-5–C-6 bond lengths obtained from the pentahydrate study. The average C-5–C-6 bond lengths are: 1.521 Å ( $\alpha$ -*gt*), 1.522 Å ( $\beta$ -*gt*), 1.524 Å ( $\alpha$ -*gg*), 1.524 Å ( $\beta$ -*gg*), and 1.535 Å for the  $\alpha$ - and  $\beta$ -*tg* conformations. This series shows for the first time the difference between the *trans* and *gauche* effect on the C-5–C-6 bond length, the *trans* or *tg* form having nearly a normal C–C bond length, while both the *gauche* forms (*gt* and *gg*) are shortened relatively independently of the water molecules surrounding this region of glucose. From our studies one can conclude that the crystal structures are biased toward the short bonds in their averages, since few *tg* conformations are observed experimentally. The interaction of water molecules tends to enhance the shortening of the C-5–C-6 bond by only  $\sim 0.002$  Å, in the  $\alpha$ -*gt* water complexes relative to the vacuum case.<sup>2</sup> On the other hand, the C-6–O-6 bond lengthening by  $\sim 0.008$  Å is only found when a hydrogen bond is formed between water and the O-6–HO-6 group; it is most probable that this through-bond interaction is partially responsible for the observed C-5–C-6 shortening upon hydration. The C-1–O-1 bond is also of interest: it was found that when the OH-1 hydrogen atom was acting as a donor, the C-1–O-1 bond was shorter than when the hydroxyl was both a donor and acceptor. The average C-1–O-1 bond lengths are: 1.409 Å ( $\alpha$ -*gt*), 1.396 Å ( $\beta$ -*gt*), 1.403 Å ( $\alpha$ -*gg*), 1.403 Å ( $\beta$ -*gg*), 1.413 Å ( $\alpha$ -*tg*), and 1.388 Å ( $\beta$ -*tg*). It is difficult to find a definite trend between the  $\alpha$  and  $\beta$  anomers for this bond, although one might suggest that some shortening occurs for the  $\beta$ -*gt* and  $\beta$ -*tg* conformers.

Discerning the hydrogen-bond energy decomposition becomes complicated with pentahydrate systems. For example, if the extra energy difference,  $\Delta E$  (total  $E$  – st mols), is considered as arising from hydrogen bonding, and there are five water molecules, one can divide this energy by five and get an estimated value of the total hydrogen-bond energy per water molecule. This is interesting but not very valuable as it does not represent the actual hydrogen-bond energy per defined hydrogen bond. There are multiple hydrogen bonds per water molecule, some as interactions with other waters, some as interactions with glucose. Furthermore, the ( $\Delta E$  (st – vac)/water) values reported include both water–water hydrogen bonding and stress on each water



molecule when their geometry differs from the in vacuo case. When all the short ( $<2.1$  Å) hydrogen bonds are counted (see Tables 1, 3, 5, 7, and 9) the average energy per hydrogen bond (considering only the water interactions) is in the range  $\sim 5$ – $9$  kcal/mol. Clearly, the glucose intramolecular interactions are changed (i.e., reduced in energy) with the intermolecular interactions with water, so it is not clear how one can correct for this change even though this energy difference appears in the glucose stress energy ( $\Delta E$  (st – vac)glucose), part of which is a result of dihedral angle deformation as well as other smaller terms. If the optimized value for the vacuum glucose conformation of interest is used and the stressed glucose value is subtracted from this value, one obtains an estimate of the loss of glucose intramolecular hydrogen-bond energy as the molecule interacts with the water. The range of stress energies for glucose run from one to 12 kcal/mol, obviously not always insignificant relative to the glucose conformational energy differences and clearly more than the relative anomeric energy difference of  $\sim 0.3$  kcal/mol.

It is of interest to examine the H–O–H angle of the 185 water molecules around glucose. Free water has an H–O–H angle of  $105.1^\circ$  at the B3LYP/6-311++G\*\* level of theory. Taking all of the water molecules on each glucose conformation, an average H–O–H angle of  $106.2^\circ$  with the minimum value of  $101.2^\circ$  and a maximum angle at  $108.1^\circ$ . The mean value lie around  $106.8^\circ$  suggesting that over all the H–O–H angle opens  $\sim 2^\circ$  upon interaction with glucose or with other water molecules. However, when we look at just the double donor (both hydrogen atoms donating) situation, the average H–O–H bond angle is in the  $101$ – $103^\circ$  range. The double donor case is unique in that the bond angle is consistently smaller than average, while a double acceptor case (only one pure double acceptor case was found) does not show any trend from the average. In one configuration,  $\beta$ -gg-II, one water is in a tetrahedral state with two donor and two acceptor interactions, and the H–O–H bond angle is again small ( $102.4^\circ$ ). The  $\sim 7^\circ$  range in H–O–H water angle is reasonable when compared to other studies we have reported where water molecules are interacting with carbohydrates<sup>1</sup> and suggests a broad vibrational frequency range for the bending mode of water, as is observed experimentally.

One must not assume that the relative free-energy terms in the tables below can be used to obtain precise anomeric ratios. The reason is that the water molecules play such a large role in the entropy terms because they are not surrounded by other water molecules and are thus very mobile and have large entropy contributions, which bias the free energy. If we instead use the zero point energy corrected total energy difference, we obtain an anomeric ratio of  $\alpha/\beta = 32/68\%$  at  $25^\circ\text{C}$ , which is in quite good agreement with experimental values. However, if we use free energy (which includes the entropy)

to calculate the anomeric ratio, we obtain a ratio,  $\alpha/\beta = 74/26\%$ , or almost the reverse of the energy-related ratio.

One goal of this study was to test our contention that water distorts the hydroxyl network of hydrogen bonds even at the optimized conditions of 0 K, and this has been supported by the results presented here. A study of glucose in solution at 300 K using empirical potentials and molecular dynamics simulations, reported that ‘the primary role of water appears to disrupt the hydrogen bonding within the carbohydrate, thereby allowing the rotamer populations to be determined by internal electronic and steric repulsions between the oxygen atoms’.<sup>31</sup> These results are in essential agreement with the conclusions presented here.

### Acknowledgements

The Biotechnology Research and Development Corporation (BRDC) is acknowledged by W.B. for grant support during a sabbatical leave.

### References

1. Momany, F. A.; Appell, M.; Strati, G.; Willett, J. L. *Carbohydr. Res.* **2004**, *339*, 553–567.
2. Appell, M.; Strati, G.; Willett, J. L.; Momany, F. A. *Carbohydr. Res.* **2004**, *339*, 537–551.
3. Melberg, S.; Rasmussen, K.; Scordamaglia, R.; Tosi, C. *Carbohydr. Res.* **1979**, *76*, 23–37.
4. Polavarapu, P. L.; Ewig, C. S. *J. Comput. Chem.* **1992**, *13*, 1255–1261.
5. Cramer, C. J.; Truhlar, D. G. *J. Am. Chem. Soc.* **1993**, *115*, 5745–5753.
6. Barrows, S. E.; Dulles, F. J.; Cramer, C. J.; French, A. D.; Truhlar, D. G. *Carbohydr. Res.* **1995**, *276*, 219–251.
7. Barrows, S. E.; Storer, J. W.; Cramer, C. J.; French, A. D.; Truhlar, D. G. *J. Comput. Chem.* **1998**, *19*, 1111–1129.
8. Salzner, U.; von Rague Schleyer, P. J. *Org. Chem.* **1994**, *59*, 2138–2155.
9. Zuccarello, F.; Buemi, G. *Carbohydr. Res.* **1995**, *273*, 129–145.
10. Brown, J. W.; Wladkowski, B. D. *J. Am. Chem. Soc.* **1996**, *118*, 1190–1193.
11. Csonka, G. I.; Elias, K.; Csizmadia, I. G. *Chem. Phys. Lett.* **1996**, *257*, 49–60.
12. Wladkowski, B. D.; Chenoweth, S. A.; Jones, K. E.; Brown, J. W. *J. Phys. Chem. A* **1998**, *102*, 5086–5092.
13. Molteni, C.; Parrinello, M. *J. Am. Chem. Soc.* **1998**, *120*, 2168–2171.
14. Lii, J.-H.; Ma, B.; Allinger, N. L. *J. Comput. Chem.* **1999**, *20*, 1593–1603.
15. Ma, B.; Schaefer, H. F., III; Allinger, N. L. *J. Am. Chem. Soc.* **1998**, *120*, 3411–3422.
16. Jebber, K. A.; Zhang, K.; Cassady, C. J.; Chung-Phillips, A. *J. Am. Chem. Soc.* **1996**, *118*, 10515–10524.
17. Jeffrey, G. A.; Pople, J. A.; Radom, L. *Carbohydr. Res.* **1972**, *25*, 117–131.
18. Hoffmann, M.; Rychlewski, J. *J. Am. Chem. Soc.* **2001**, *123*, 2308–2316.

19. Corchado, J. C.; Sanchez, M. L.; Aquilar, M. A. *J. Am. Chem. Soc.* **2004**, *126*, 7311–7319.
20. Hemmingsen, L.; Madsen, D. E.; Esbensen, A. L.; Olsen, L.; Engelsen, S. B. *Carbohydr. Res.* **2004**, *339*, 937–948.
21. Jockusch, R. A.; Kroemer, R. T.; Talbot, F. O.; Simons, J. P. *J. Phys. Chem. A* **2003**, *107*, 10725–10732.
22. Hollenberg, J. L.; Hall, D. O. *J. Phys. Chem.* **1983**, *87*, 695–696.
23. Momany, F. A.; Willett, J. L. *Carbohydr. Res.* **2000**, *326*, 194–209.
24. Momany, F. A.; Willett, J. L. *Carbohydr. Res.* **2000**, *326*, 210–226.
25. Becke, A. D. *J. Chem. Phys.* **1993**, *98*, 5648.
26. For the performance of B3LYP with a split valence basis set used to calculate interaction energies see, for example, (a) Novoa, J. J.; Sosa, C. *J. Phys. Chem.* **1995**, *99*, 15837; (b) Csonka, G. I.; Elias, K.; Csizmadia, I. G. *Chem. Phys. Lett.* **1996**, *257*, 49; (c) Sirois, S.; Proynov, E. I.; Nguyen, D. T.; Salahub, D. R. *J. Chem. Phys.* **1997**, *107*, 6770; (d) Barrows, S. E.; Storer, J. W.; Cramer, C. J.; French, A. D.; Truhler, D. G. *J. Comput. Chem.* **1998**, *19*, 1111; (e) Paizs, B.; Suhai, S. *J. Comput. Chem.* **1998**, *19*, 575; (f) Hagemester, F. C.; Gruenloh, C. J.; Zwier, T. S. *J. Phys. Chem. A* **1998**, *102*, 82; (g) Ma, B.; Schaefer, H. F., III; Allinger, N. *J. Am. Chem. Soc.* **1998**, *120*, 3411.
27. Momany, F. A.; Willett, J. L. *J. Comput. Chem.* **2000**, *21*, 1204–1219.
28. Strati, G.; Willett, J. L.; Momany, F. A. *Carbohydr. Res.* **2002**, *337*, 1833–1849.
29. Strati, G.; Willett, J. L.; Momany, F. A. *Carbohydr. Res.* **2002**, *337*, 1851–1859.
30. PQS Ab Initio Program Package, Parallel Quantum Solutions, 2013 Green Acres, Suite E, Fayetteville, AR 72703, USA.
31. Kirschner, K. N.; Woods, R. J. *Proc. Natl. Acad. Sci. U.S.A.* **2001**, *98*, 10541–10545.